J. Inst. Math. Jussieu (2024), **23**(6), 2441–2459
doi:10.1017/S1474748023000543

CHARACTERIZATION OF THE REDUCED PERIPHERAL SYSTEM OF LINKS

BENJAMIN AUDOUX[1] AND JEAN-BAPTISTE MEILHAN[2]

[1] *Aix-Marseille Univ., CNRS, Centrale Marseille, I2M, Marseille, France*
(benjamin.audoux@univ-amu.fr)

[2] *Univ. Grenoble Alpes, CNRS, Institut Fourier, F-38000 Grenoble, France*
(jean-baptiste.meilhan@univ-grenoble-alpes.fr)

(Received 14 March 2022; revised 8 December 2023; accepted 11 December 2023; first published online 1 February 2024)

Abstract The reduced peripheral system was introduced by Milnor [18] in the 1950s for the study of links up to link-homotopy, that is, up to homotopies leaving distinct components disjoint; this invariant, however, fails to classify links up to link-homotopy for links of four or more components. The purpose of this paper is to show that the topological information which is detected by Milnor's reduced peripheral system is actually 4-dimensional. The main result gives indeed a complete characterization of links having the same reduced peripheral system, in terms of ribbon solid tori in 4–space up to ribbon link-homotopy. The proof relies on an intermediate characterization given in terms of welded diagrams up to self-virtualization, hence providing a purely topological application of the combinatorial theory of welded links.

Introduction

It is known since Dehn's work in 1914 that the capacity of the fundamental group of link complements to separate links can be improved by looking at some specific elements; the right and left trefoils, although having isomorphic groups, can be distinguished by their meridian-longitude pairs. But it is only in the 1950s that Fox formalized the notion of *peripheral system* for links, which is the fundamental group endowed with the data, for each component of a link L in S^3, of a pair of elements $\{m_i,l_i\}$ of $\pi_1(S^3 \setminus L)$—a meridian and a preferred longitude—that generates the fundamental group of the corresponding boundary component of $S^3 \setminus L$. Although rather intractable in practice, the peripheral system is nonetheless an essential link invariant which has been, 15 years later, proved to be complete by Waldhausen [21]. It is natural to expect that some

Key words and phrases: classical links; welded links; ribbon surfaces; reduced peripheral systems; self-virtualization

2020 Mathematics subject classification: Primary 57K10; 57K12

weaker equivalence relations than ambient isotopy could be classified by an appropriate adaptation of the peripheral system. As early as the 1950s, this has been the strategy of Milnor in his attempt to classify links up to *link-homotopy* [18], that is, up to homotopy deformations during which distinct connected components remain disjoint at all times. In order to address this link-homotopy classification problem, Milnor introduced the *reduced peripheral system*. Roughly speaking, the *reduced fundamental group* $R\pi_1(L^c)$ of a link L is the largest quotient of the fundamental group of the complement where any generator commutes with any of its conjugates; if $\{\mu_i,\lambda_i\}_i$ is a peripheral system for L, with image $\{m_i,l_i\}_i$ under the projection onto $R\pi_1(L^c)$, then a *reduced peripheral system* of L is $\{m_i,l_iN_i\}_i$, where N_i is the normal subgroup of $R\pi_1(L^c)$ generated by m_i. The reduced peripheral system, however, only yields a complete link-homotopy invariant for links with at most three components. The 4-component case was tackled by Levine [16] only 40 years later, using a smaller normal subgroup for defining the reduced longitudes. As a matter of fact, there exists a pair of 4-component links, exhibited by Hughes, with equivalent reduced peripheral systems but which are link-homotopically distinct [13]. It seems still unknown whether Levine's [16] peripheral system classifies links up to link-homotopy. In fact, this classification was achieved by Habegger and Lin by a rather different approach, which relies on representing links as the closure of string links [12]. Extracted from the reduced peripheral system, (nonrepeating) Milnor numbers were also introduced in [18]; they are defined, up to some indeterminacy, as the coefficients in the Magnus expansion of longitudes. Milnor showed that these numbers also classify links with up to three components, up to link-homotopy. In [8], these numbers were shown to be closely related to 4-dimensional topology, through the notion of twisted Whitney towers. The purpose of the present paper is to show that the whole reduced peripheral system actually also arises from 4-dimensional topology. We make use of the theory of welded links to provide in an elementary way a 4-dimensional topological characterization of the information captured by Milnor's reduced peripheral system:

Main Theorem. *Let L and L' be two oriented links in the 3-sphere. The following are equivalent:*

i. *L and L' have equivalent reduced peripheral systems;*
ii. *L and L' are sv-equivalent, as welded links;*
iii. *$\mathrm{Spun}^\bullet(L)$ and $\mathrm{Spun}^\bullet(L')$ are ribbon link-homotopic, as ribbon immersed solid tori.*

Here, *welded links* are generalized link diagrams, where we allow virtual crossings in addition to the usual crossings, regarded up to an extended set of Reidemeister moves. These welded links can be regarded as a generalization of classical links, as there is an injective map sending the former inside the set of the latter; and the fundamental group and (reduced) peripheral system actually extend to this larger class of objects. This theory takes its origins in the late 1990s [10] and has experienced some important developments in the past decade (see, for instance [4, 5, 6, 7, 9, 17, 20] and references therein). Part ii then gives a diagrammatic characterization of the reduced peripheral systems of links, by regarding them as welded links via their diagrams, up to sv-*equivalence*, which is the equivalence relation generated by the replacement of a classical crossing involving

https://doi.org/10.1017/S1474748023000543 Published online by Cambridge University Press

two strands of a same component by a virtual one; this stresses, in particular, the fact that the sv-equivalence is a refinement of link-homotopy for classical links (see Remark 1.6). This characterization actually follows from a more general result, which classifies all welded links up to sv-equivalence (see Theorem 2.1). Also, it follows that the non link-homotopic 4-component links exhibited by Hughes in [13] are sv-equivalent; this is made explicit in Appendix.

Part iii gives a topological characterization of the reduced peripheral system, in terms of 4-dimensional topology. A classical construction dating back to Artin [1] produces a knotted surface in 4-space from a link in 3-space by spinning it around some plane. By spinning as well projection rays from the link to the plane, this can be extended to a map $\mathrm{Spun}^\bullet$ producing *ribbon-immersed solid tori*, *that is,* solid tori in 4-space intersecting along only ribbon singularities. The *ribbon link-homotopy* for such objects is a notion of homotopy within the realm of ribbon-immersed solid tori, which induces a link-homotopy for the boundary, allowing the removal/insertion of such ribbon singularities inside the same connected component. The reduced peripheral system for links hence appears in this way as an intrinsically 4-dimensional invariant, rather than a 3-dimensional one.[1] As above, this characterization is obtained as a consequence of a more general result, characterizing the reduced peripheral system of welded links in terms of 4-dimensional topology (see Theorem 3.7). It is thus noteworthy that our purely topological characterization i $\Leftrightarrow$ iii for classical links is actually obtained as an application of virtual/welded knot theory.

1. The reduced peripheral system of classical and welded links

1.1. Welded links

In this section, we review the theory of welded links and Gauss diagrams.

Definition 1.1.

- An n-component *welded diagram* is a planar immersion of n ordered and oriented circles, whose singular set is a finite number of transverse double points, each double point being labelled either as a *positive or negative (classical) crossing*, or as a *virtual crossing*:

- We denote by $w\mathcal{L}_n$ the set of n-component welded diagrams up to planar isotopy, classical Reidemeister moves R1, R2, and R3, which are the three usual moves of classical knot theory, and the following *welded moves*[2]:

[1] One might expect for this 4-dimensional incarnation to be in terms of knotted surfaces, we explain in Section 3.3 why this is not the case.

[2] Here, OC stands for *over-commute*, as a strand is passing over a virtual crossing; note that the corresponding *under-commute* move is forbidden.

https://doi.org/10.1017/S1474748023000543 Published online by Cambridge University Press

virtual Reidemeister moves

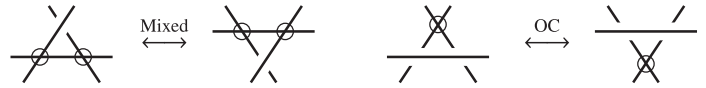

Mixed and OC moves

Elements of $w\mathcal{L}_n$ are called *welded links*.

A welded diagram with no virtual crossing is called *classical*. It is well-known that this set-theoretical inclusion induces an injection of the set $\mathcal{L}_n$ of n-component classical link diagrams up to classical Reidemeister moves, into $w\mathcal{L}_n$; as pointed out in Remark 1.13, this follows from the fact that the peripheral system is a complete link invariant.

An alternative approach to welded links, which is often more tractable in practice, is through the notion of Gauss diagrams.

Definition 1.2. An n-component *Gauss diagram* is the homeomorphism class of an abstract collection of n ordered and oriented circles, together with disjoint signed arrows whose endpoints are pairwise disjoint points of these circles. For each arrow, the two endpoints are called *head* and *tail*, with the obvious convention that the arrow orientation goes from the tail to the head.

To a welded diagram corresponds a unique Gauss diagram, given by joining the two preimages of each classical crossing by an arrow, oriented from the overpassing to the underpassing strand and labelled by the crossing sign. See below for an example:

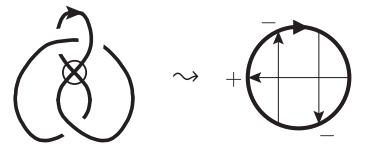

Definition 1.3. Two Gauss diagrams are *welded equivalent* if they are related by a sequence of the following *welded moves*:

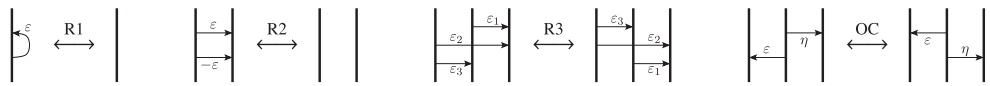

where move R3 requires the additional sign condition that $\varepsilon_2\varepsilon_3 = \tau_2\tau_3$, where $\tau_i = 1$ if the i^{th} strand (from left to right) is oriented upwards, and -1 otherwise.

As the notation suggests, these four moves are just the Gauss diagram analogues, using the above correspondance, of the three classical Reidemeister moves and the OC move

https://doi.org/10.1017/S1474748023000543 Published online by Cambridge University Press

for welded diagrams (the Gauss diagram versions of the virtual Reidemeister and Mixed moves being trivial). As a matter of fact, it is easily checked that welded equivalence classes of Gauss diagrams are in one-to-one correspondence with welded links.

Remark 1.4. We will make use of the following *Slide* move

which is easily seen to follow from the R2, R3, and OC moves. Note that this is a Gauss diagram analogue of the Slide move on arrow diagrams [17].

In a welded diagram, a *self-crossing* is a crossing where both preimages belong to the same component.

Definition 1.5. A *self-virtualization* is a local move SV, illustrated below, which replaces a classical self-crossing by a virtual one. The sv-*equivalence* is the equivalence relation on welded diagrams generated by self-virtualizations

At the Gauss diagram level, a self-crossing is represented by a *self-arrow*, that is an arrow whose endpoints lie on the same component, and a self-virtualization move simply erases a self-arrow.

Remark 1.6. The link-homotopy relation for classical links, as defined by Milnor, is generated by the self-crossing change, *that is,* the local move that exchanges the relative position of two strands of a same component. As the left-hand side of the above picture suggests, a self-crossing change can be realized by two self-virtualizations, and the sv-equivalence is thus a refinement of the link-homotopy relation for classical links. In [4], self-virtualization was proven to actually extend classical link-homotopy for string links, in the sense that two string-links are sv-equivalent if and only if they are link-homotopic. Our main theorem, together with Hughes's [13] counter-examples, shows that such an equivalence does not hold true for links.

We end this section with a normal form for Gauss diagrams up to self-virtualization.

Definition 1.7. A Gauss diagram is *sorted* if each circle splits into two arcs, the t- and the h-arc, containing, respectively, tails only and heads only.

Remark 1.8. Up to OC moves, a sorted Gauss diagram D is uniquely determined by the data of n words $\left\{\prod_{j=1}^{k_i}\mu_{s_{ij}}^{\varepsilon_{ij}}\right\}_i$ in the alphabet $\{\mu_1^{\pm 1},\ldots,\mu_n^{\pm 1}\}$, where the letter $\mu_{s_{ij}}^{\varepsilon_{ij}}$ indicates that the j^{th} head met on C_i when running along its oriented h–arc is connected by an ε_{ij}–signed arrow to one of the tails on $C_{s_{ij}}$.

https://doi.org/10.1017/S1474748023000543 Published online by Cambridge University Press

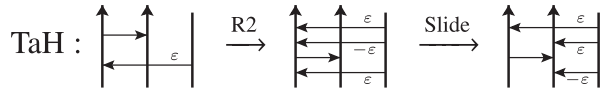

Figure 1. Tail across head move on Gauss diagrams.

Lemma 1.9. *Every Gauss diagram is sv-equivalent to a sorted one.*

Proof. Start with any given Gauss diagram, and choose any arbitrary order on the circles to sort them one by one as follows. Using SV moves, remove first all self-arrows from the considered circle, and then gather all heads located on it using tail across head (TaH) moves, described in Figure 1. Since there is no self-arrow left on the considered circle, the two extra arrows appearing in the latter moves won't have endpoints on the considered circle, and as their heads, respectively, tails, are adjacent to the already existing arrow head, respectively, tail, this won't unsort already sorted components. Note that these two extra arrows could happen to be self-arrows, but this does not conflict with the sorting procedure.

□

1.2. Welded link groups and peripheral systems

Let L be a welded diagram.

Definition 1.10.

- The *arcs* of L are the maximal pieces of L which do not underpass any classical crossing. An arc is hence either a whole component or a piece of strand which starts and ends at some (possibly the same) crossings; it might pass through some virtual crossings and overpass some classical ones. At the level of Gauss diagrams, an arc corresponds to portions of circles comprised between two heads.
- The *group of* L, denoted by $G(L)$, is defined by a Wirtinger-type presentation, where each arc yields a generator, and each classical crossing yields a relation, as follows:

Since virtual crossings do not produce extra generators or relations, it is clear that virtual Reidemeister moves and Mixed moves preserve the group presentation. It is also easily checked that the isomorphism class of this group is invariant under classical Reidemeister and OC moves and is thus an invariant of welded links [14, 20]. If L is a diagram of a classical link $\mathcal{L}$, then $G(L)$ is the fundamental group of the complement of an open tubular neighborhood of $\mathcal{L}$ in S^3; in this case, an arc corresponds to the topological meridian which positively enlaces it. By analogy, arcs of welded diagrams can be seen as some combinatorial meridians, and we will often blur the distinction between arcs/meridians of L and the corresponding generators of $G(L)$. We will also regularly, and

https://doi.org/10.1017/S1474748023000543 Published online by Cambridge University Press

sometimes implicitly, make use of the simple fact that two meridians of a same component are always conjugate.

Definition 1.11.

- A *basing* of L is a choice of one meridian for each component of L.
- For each i, the *ith preferred longitude* of L with respect to the basing $\{\mu_1,\dots,\mu_n\}$ is the element $\lambda_i \in G(L)$ obtained as follows: when running along the ith component of L, starting at the arc labelled by μ_i and following the orientation, write ω^{ε} when passing under an arc labelled by ω at a classical crossing of sign ε, and finally write μ_i^{-k}, where k is the algebraic number of classical self-crossings in the ith component.
- A *peripheral system* for L is the group $G(L)$ endowed with the choice of a basing and the data, for each i, of the ith preferred longitude.

When L is a classical link, a basing is the choice of a topological meridian for each component, and the ith preferred longitude represents a parallel copy of the ith component having linking number zero with it. Hence, the above definitions naturally generalize the usual notion of peripheral system of links.

Two peripheral systems $\big(G,\{(\mu_i,\lambda_i)\}_i\big)$ and $\big(G,\{(\mu'_i,\lambda'_i)\}_i\big)$ are *conjugate* if, for each i, there exists $\omega_i \in G$, such that $\mu'_i = \omega_i^{-1}\mu_i\omega_i$ and $\lambda'_i = \omega_i^{-1}\lambda_i\omega_i$. Two peripheral systems $(G,\{(\mu_i,\lambda_i)\}_i)$ and $(G',\{(\mu'_i,\lambda'_i)\}_i)$ are *equivalent* if there exists an isomorphism $\psi : G' \to G$, such that $\big(G,\{(\mu_i,\lambda_i)\}_i\big)$ and $\big(G,\{(\psi(\mu'_i),\psi(\lambda'_i))\}_i\big)$ are conjugate.

The following is well-known (see, for example [15, Proposition 6].

Lemma 1.12. *Up to conjugation, peripheral systems are well-defined for welded diagrams and yield, up to equivalence, a well-defined invariant of welded links.*

Proof. Suppose that $\{(\mu_i,\lambda_i)\}_i$ is a peripheral system of the welded diagram L, and let μ'_i be another choice of meridian for the ith component, yielding hence another preferred ith longitude λ'_i. Then, $\mu'_i = \omega_i^{-1}\mu_i\omega_i$ for some $\omega_i \in G(L)$, and by definition, $\lambda'_i = \omega_i^{-1}(\lambda_i\mu_i^k)\omega_i{\mu'_i}^{-k}$. But substituting μ'_i for $\omega_i^{-1}\mu_i\omega_i$ in λ'_i then gives $\lambda'_i = \omega_i^{-1}\lambda_i\mu_1^k\omega_i\omega_i^{-1}\mu_i^{-k}\omega_i = \omega_i^{-1}\lambda_i\omega_i$. This proves that the peripheral system of L is uniquely determined up to conjugation.

Using this fact, it is then an easy exercise to check that equivalence classes of peripheral systems are well-defined for welded links, *that is,* that they are invariant under welded and classical Reidemeister moves. More precisely, by an appropriate choice of basing, one can check that each classical Reidemeister move induces an isomorphism of the groups of the diagrams which preserves each preferred longitude; the argument is even simpler for welded Reidemeister moves.

As an elementary illustration, let us consider two welded diagrams L and L' which differ by an R1 move, as shown below. The generators α and β of $G(L)$ shown in the figure satisfy $\alpha = \beta$, so $G(L)$ and $G(L')$ are clearly isomorphic. Pick $\beta \in G(L)$, respectively, $\alpha \in G(L')$, as meridian for the depicted component of L, respectively, L'.

https://doi.org/10.1017/S1474748023000543 Published online by Cambridge University Press

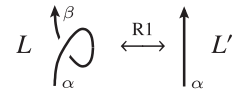

Then the corresponding preferred longitude of L is of the form $\omega\alpha\alpha^{-k}$ for some $\omega \in G(L)$ and some $k \in \mathbb{Z}$, while the corresponding preferred longitude of L' reads $\omega\alpha^{-k+1}$, since L' contains one less positive self-crossing. Hence, the above isomorphism from $G(L)$ to $G(L')$ preserves the peripheral system. □

Remark 1.13. The peripheral system of classical links is a complete invariant [21]. Since this invariant extends to welded links, in the sense that the above-defined invariant coincides with the usual peripheral system for classical links, this shows the known fact [11, 14] that the natural map from classical links to welded links is injective.

1.3. Reduced group and reduced peripheral system

As before, let us consider a welded diagram L.

Definition 1.14. For a group G given with a finite generating set X, the *reduced group of* G, denoted by $\mathrm{R}G$, is the quotient of G by its normal subgroup generated by all elements $[\zeta,\omega^{-1}\zeta\omega]$, where $\zeta \in X$ and $\omega \in G$. In particular, we define the *reduced group of* L as the reduced group $\mathrm{R}G(L)$ of $G(L)$ with respect to its Wirtinger generators.

Note that $\mathrm{R}G(L)$ is the largest quotient of $G(L)$ where any meridian commutes with any of its conjugates. Since any two meridians of a same component are conjugate elements, it can also be defined as the quotient of $G(L)$ by the normal subgroup generated by the elements $[\mu_i,\omega^{-1}\mu_i\omega]$ for all $\omega \in G(L)$, where $\{\mu_i\}_i$ is a fixed basing for L.

Convention. In the rest of this paper, we shall use Greek letters with tilde for elements in the group of a welded diagram, and use the same letters, but without the tilde, to denote the corresponding elements in the reduced group. In particular, we respectively denote by μ_i and λ_i the images in $\mathrm{R}G(L)$ of any meridian $\widetilde{\mu}_i$ and longitude $\widetilde{\lambda}_i$ in $G(L)$.

Definition 1.15. The *reduced peripheral system* for L are the data

$$\big(\mathrm{R}G(L),\{(\mu_i,\lambda_i.N_i)\}_i\big),$$

associated to a peripheral system $\big(G(L),\{(\widetilde{\mu}_i,\widetilde{\lambda}_i)\}_i\big)$, where, for each i, $\lambda_i.N_i$ denotes the coset of λ_i, with respect to N_i, the normal subgroup generated by the ith reduced meridian μ_i. Two reduced peripheral systems are *conjugate* if they come from conjugate peripheral systems; and they are *equivalent* if there is a group isomorphism sending one to a conjugate of the other.

As explained in the Introduction, Milnor introduced the reduced peripheral system for classical links and showed that it is a link-homotopy invariant. We have the following generalization.

Lemma 1.16. *Up to equivalence, the reduced peripheral system is a well-defined invariant of welded links up to sv-equivalence.*

https://doi.org/10.1017/S1474748023000543 Published online by Cambridge University Press

Proof. Since equivalent peripheral systems obviously yield equivalent reduced peripheral systems, it suffices to prove the invariance under a single SV move. Pick a self-crossing s of some welded diagram L, and denote by L_s the diagram obtained by replacing s by a virtual crossing:

Consider the three generators $\widetilde{\alpha},\widetilde{\beta},\widetilde{\gamma}$ of $G(L)$ involved in s, as shown above. Since the meridians $\widetilde{\alpha}$, $\widetilde{\beta}$, and $\widetilde{\gamma}$ all belong to the same component, there are $\widetilde{\omega},\widetilde{\zeta} \in G(L)$, such that $\widetilde{\beta} = \widetilde{\omega}^{-1}\widetilde{\alpha}\widetilde{\omega}$ and $\widetilde{\alpha} = \widetilde{\zeta}^{-1}\widetilde{\gamma}\widetilde{\zeta}$. For L, the Wirtinger relation at s is $\widetilde{\gamma} = \widetilde{\alpha}^{-1}\widetilde{\beta}\widetilde{\alpha}$; hence, we have that $\gamma = \alpha^{-1}\omega^{-1}\alpha\omega\alpha \equiv \omega^{-1}\alpha\omega = \beta$ holds in $\mathrm{R}G(L)$, which shows that $\mathrm{R}G(L)$ is isomorphic to $\mathrm{R}G(L_s)$.

It remains to show that this isomorphism preserves the reduced peripheral system. Pick $\widetilde{\alpha} \in G(L)$ as meridian $\widetilde{\mu}$ for the component of L containing s; the corresponding preferred longitude is given by $\widetilde{\lambda} = \widetilde{\omega}\widetilde{\alpha}\widetilde{\zeta}\widetilde{\alpha}^{-k}$ for some integer k. Take the meridian $\widetilde{\mu}_s$ of the corresponding component of L_s to be represented by $\widetilde{\alpha}$ again, so that the preferred longitude is given by $\widetilde{\lambda}_s = \widetilde{\omega}\widetilde{\zeta}\widetilde{\alpha}^{-k+1}$. Then the isomorphism $\mathrm{R}G(L) \to \mathrm{R}G(L_s)$ maps μ to μ_s, and the equality

$$\lambda = \omega\alpha\zeta\alpha^{-k} \equiv \omega[\zeta,\alpha]\alpha\zeta\alpha^{-k} = \omega\zeta\alpha\zeta^{-1}\alpha^{-1}\alpha\zeta\alpha^{-k} = \omega\zeta\alpha^{-k+1} \pmod{N}$$

shows that $\lambda.N$ is mapped to $\lambda_s.N_s$, where $N \subset \mathrm{R}G(L)$ and $N_s \subset \mathrm{R}G(L_s)$ denote the normal subgroups generated by α. This handles one version of the SV move, but the other one is strictly similar. □

Remark 1.17. Since we are overall working modulo the normal subgroup generated by the meridian α, the above sequence of equalities for the longitude λ could be slightly simplified. It seems, however, instructive to point out that one only needs to consider this normal subgroup in the second equality of this sequence; this identifies precisely where this equivalence is needed to have the desired invariance property.

In particular, the reduced fundamental group is hence invariant under self-virtualization. Combining this with the sorted form given in Lemma 1.9, we obtain the following presentation.

Lemma 1.18. *The reduced fundamental group $RG(L)$ has the following presentation*

$$RG(L) = \big\langle \mu_1,\dots,\mu_n \;\big|\; [\mu_i,\lambda_i], [\mu_i,\omega^{-1}\mu_i\omega], \text{ for all } i \text{ and for all } \omega \in F(\mu_i) \big\rangle,$$

where $F(\mu_i)$ denotes the free group on $\{\mu_i\}_i$.

Proof. Suppose first that L corresponds to a sorted Gauss diagram. The Wirtinger-type presentation for its welded link group provides, for every component C_i, a generator μ_i corresponding to the t–arc, and a bunch of generators μ_i^j lying on the h–arc. Any of the latter appears in exactly two relations which are of the form $\mu_i^j = \mu_{i_1}^{\pm 1}\mu_i^{j-1}\mu_{i_1}^{\mp 1}$ and $\mu_i^{j+1} = \mu_{i_2}^{\pm 1}\mu_i^j\mu_{i_2}^{\mp 1}$, setting $\mu_i^0 := \mu_i =: \mu_i^{r_i}$ where r_i is the number of heads on C_i;

https://doi.org/10.1017/S1474748023000543 Published online by Cambridge University Press

generators μ_i^j can hence be successively eliminated, ending with relations $[\mu_i,\lambda_i]$ only. Hence, the presentation

$$G(L) = \langle \mu_1,\dots,\mu_n \mid [\mu_i,\lambda_i],\ \text{for all } i\rangle.$$

Relations $[\mu_i,\omega^{-1}\mu_i\omega]$ then naturally arise when taking the reduced quotient. The general case, where L does not necessarily correspond to a sorted Gauss diagram, then follows readily from Lemmas 1.9 and 1.16. □

Remark 1.19. Starting with a sorted Gauss diagram D, Lemma 1.18 provides a presentation for the associated reduced fundamental group whose generators $\{\mu_i\}_i$ correspond to the t–arcs, and whose relations make these generators commute with their own conjugates, as well as with their associated longitude. Moreover, as words in the generators, these longitudes are directly given by the words associated to D in Remark 1.8. Conversely, any such presentation provides a word representative for each longitude and hence describes, up to OC moves, a unique sorted Gauss diagram.

Remark 1.20. Lemma 1.18 is to be compared with [19, Theorem 4], where Milnor gives a similar presentation for the nilpotent quotients of the group of a classical link. Actually, Milnor's argument being purely algebraic, the proof of [19, Theorem 4] applies verbatim to the case of welded links, meaning, in particular, that the nilpotent quotient $G(L)/\Gamma_k G(L)$ has a presentation $\langle \mu_1,\dots,\mu_n \mid \Gamma_k F(\mu_i), [\mu_i,\lambda_i] \text{ for all } i\rangle$. In fact, Milnor's proof can be adapted with minor adjustments to give an alternative proof of Lemma 1.18.

2. Diagrammatic characterization of the reduced peripheral system

This section is devoted to the proof of the following result, which readily implies the equivalence i $\Leftrightarrow$ ii in our main theorem, and which more generally classifies welded links up to sv-equivalence.

Theorem 2.1. *Two welded links are sv-equivalent if and only if they have equivalent reduced peripheral systems.*

For convenience, we will adopt here the Gauss diagram point of view. Fix a number $n \in \mathbb{N}^*$ of components, and set $\mathrm{F}(\mu_i)$ the free group over elements $\mu_1,\dots,\mu_n$.

Proof. The "only if" part of Theorem 2.1 was proved in Lemma 1.16. Conversely, let L and L' be two welded diagrams with equivalent reduced peripheral systems $\big(\mathrm{R}G(L),\{(\mu_i,\lambda_i.N_i)\}_i\big)$ and $\big(\mathrm{R}G(L'),\{(\mu'_i,\lambda'_i.N'_i)\}_i\big)$.

We may assume, using Lemma 1.9, that L and L' are both given by sorted Gauss diagrams D and D'. Using Remarks 1.8 and 1.19, we may further assume that the λ_i's and the λ'_i's are represented by the words in, respectively, the μ_j's and the μ'_j's, given by D and D'. Following Remark 1.19, the strategy will be to apply welded and SV moves on D' to produce a diagram whose associated presentation for the reduced fundamental group is the same as the one of D. To keep notation light, we will still denote by D', μ'_i, and λ'_i all the sorted Gauss diagrams, generators for the reduced fundamental group, and representative words for the longitudes, successively obtained after modifications.

https://doi.org/10.1017/S1474748023000543 Published online by Cambridge University Press

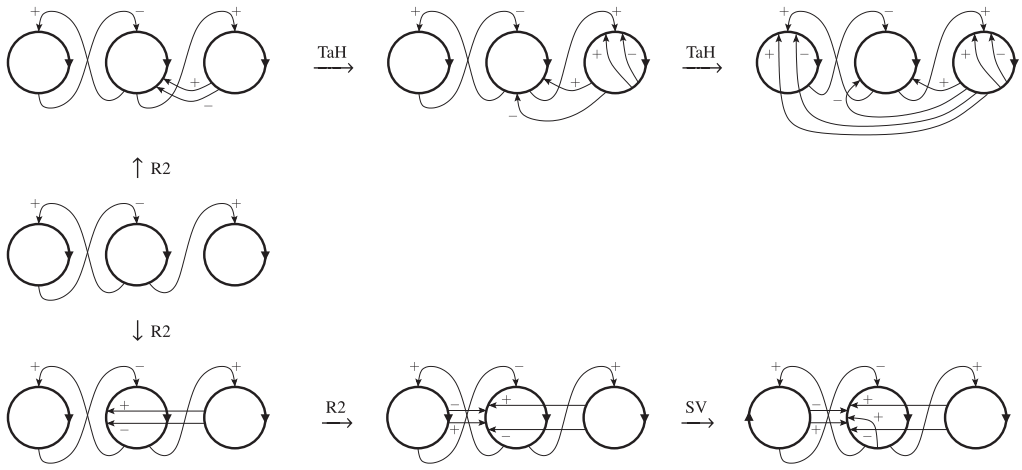

Figure 2. Making the equivalence an isomorphism.

To begin, we first modify D' so that the isomorphism $\psi : \mathrm{R}G(L') \to \mathrm{R}G(L)$ sends each pair (μ'_i,λ'_i) to (μ_i,λ_i). Algebraically, transforming $\psi(\mu'_i,\lambda'_i)$ into (μ_i,λ_i) can be achieved in two steps:

(1) since $\psi(\mu'_i)$ is a conjugate of μ_i, perform a sequence of "elementary conjugations", each replacing both μ'_i and λ'_i by their conjugate by ${\mu'_j}^{\varepsilon}$, for some index $j \neq i$ and some sign ε, so that $\psi\big((\mu'_i,\lambda'_i.N'_i)\big) = (\mu_i,\lambda_i.N_i)$. Indeed, since, for any words g_1 and g_2, $\mu_i^{g_1\mu_i g_2}$ and $\mu_i^{g_1 g_2}$ are equal in the reduced quotient, and $\lambda_i^{g_1\mu_i g_2}$ and $\lambda_i^{g_1 g_2}$ are congruent modulo N_i, all occurrences of μ_i in the conjugating element can be removed;

(2) since $\psi(\lambda'_i)$ is an element of $\lambda_i.N_i$, multiply λ'_i by an appropriate product of conjugates of ${\mu'_i}^{\pm 1}$, so that $\psi(\lambda'_i) = \lambda_i$.

These two steps have to be realized at the diagrammatical level:

(1) for each elementary conjugation, use R2 to add two parallel arrows going from the jth t-arc to the starting endpoint of the ith t-arc, and then pull the head of the $(-\varepsilon)$-labelled arrow along the ith t–arc using the TaH move given in Figure 1. This yields an equivalent Gauss diagram which is still sorted, and which realizes the desired elementary conjugation. See the upper half of Figure 2 for an example where μ'_2 and λ'_2 are conjugated by μ'_3, the components being numbered from left to right;

(2) to add a conjugate $g{\mu'_i}^{\pm 1}g^{-1}$ of ${\mu'_i}^{\pm 1}$ to λ'_i, use repeatedly R2 to add the trivial word gg^{-1} to the ith longitude of D', and then a single SV move to produce the desired word $g{\mu'_i}^{\pm 1}g^{-1}$. See the lower half of Figure 2 for an example where the conjugate of μ'_2 by ${\mu'_1}^{-1}\mu'_3$ is introduced in λ'_2, the components being numbered from left to right.

https://doi.org/10.1017/S1474748023000543 Published online by Cambridge University Press

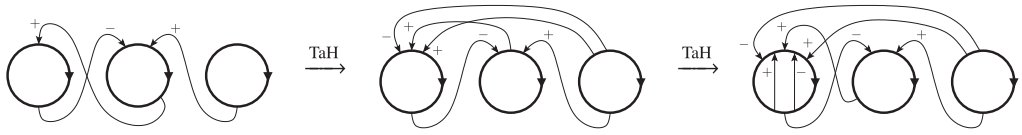

Figure 3. Conjugating meridian factors in longitudes.

We have thus realized the isomorphism $\psi : \mathrm{R}G(L') \to \mathrm{R}G(L)$ which sends each μ'_i to μ_i, and each λ'_i to λ_i. As a matter of fact, we can now identify μ'_i with μ_i. We will now modify D' component by component in order to transform it into D. For the ith step, we first note that λ_i and λ'_i are equal in $\mathrm{R}G(L)$; following the presentation of $G(L')$ given by Lemma 1.18 on D' (as it stands at the end of the $(i-1)$th step), λ_i can be obtained from λ'_i by performing a finite sequence of the following moves:

i. $\mu_j^{\pm 1}\mu_j^{\mp 1} \leftrightarrow 1$;
ii. $\mu_j^{\pm 1} \to {\lambda'_j}^{-1}\mu_j^{\pm 1}\lambda'_j$;
iii. $\omega\mu_j^{\pm 1} \to \mu_j^{\pm 1}\omega$, where ω is of the form $\zeta^{-1}\mu_j^{\pm 1}\zeta$ with $\zeta \in \mathrm{F}(\mu_i)$.

Each of these moves can be diagrammatically realized on D'. Relations i correspond indeed to R2 moves. For Relations ii and iii, we first address the $j = i$ case by noting that we can actually realize the more general move $\omega\mu_i^{\pm 1} \to \mu_i^{\pm 1}\omega$ with $\omega \in \mathrm{F}(\mu_i)$, as follows. Note that the $\mu_i^{\pm}$ term corresponds to a self-arrow: it can hence be removed from one side of ω and reinserted on the other side using SV moves. Let us now consider Relations ii and iii with $j \neq i$. For Relations ii, the term $\mu_j^{\pm 1}$ corresponds this time to an arrow a whose tail sits on the jth component; moving this tail along the whole circle component, against the orientation, does conjugate $\mu_j^{\pm 1}$ by λ'_j. Indeed, using TaH moves, the tail of a will cross every head on its way at the cost of conjugating the head of a with the desired arrows; see Figure 3 for an example where the μ_2 factor in λ'_1 is conjugated by λ'_2, the components being numbered from left to right.

Finally, Relations iii can be handled exactly as in the proof of [4, Lemma 4.26]. Once all components have been processed, D' is transformed into D, showing that $L' = L$ as welded links. □

3. A topological characterization of the reduced peripheral system

Welded links are closely related to *ribbon knotted tori* and *ribbon solid tori* in S^4, and the characterization of classical links having the same reduced peripheral systems given by Theorem 2.1 can be recasted in terms of 4-dimensional topology.

3.1. The enhanced Spun map

Given a classical link $L \subset \mathbb{R}^3$, a well-known procedure to construct ribbon knotted tori in 4-space is to take the *Spun* of L: consider a plane $\mathcal{P}$ which is disjoint from a 3-ball containing L, and spin L around $\mathcal{P}$ inside $\mathbb{R}^4 \supset \mathbb{R}^3$. The result is a union of knotted tori, which we denote by $\mathrm{Spun}(L)$. If the projection $D(L,\mathcal{P})$ of L onto the plane $\mathcal{P}$ is regular,

https://doi.org/10.1017/S1474748023000543 Published online by Cambridge University Press

then spinning as well the orthogonal projection rays from L to $\mathcal{P}$ provides immersed solid tori whose boundary is $\mathrm{Spun}(L)$ and whose singularities are so-called *ribbon* disks, corresponding to the crossings of $D(L,\mathcal{P})$. Of course, this *ribbon filling* depends on the choice of plane $\mathcal{P}$, and more precisely on the diagram $D(L,\mathcal{P})$, which may be changed by some sequence of Reidemeister moves. But for each Reidemeister move, there is an associated singular diagram, that is, a singular plane $\mathcal{P}_s$, and spinning L around $\mathcal{P}_s$ provides some singular ribbon filling which can be infinitesimally desingularized into the spun of one or the other side of the Reidemeister move. This leads to the following definitions, which settles a notion of (singular) ribbon solid tori.

Definition 3.1. Let $\varphi : M \to S^4$ be an immersed 3-dimensional manifold. Let D be a connected component of the singular set of $\varphi(M)$ contained in an open 4-ball $B \subset S^4$. We say that D is a *ribbon singularity*:[3]

- *of type* 0 if $\varphi^{-1}(B)$ is the disjoint union $B_1 \sqcup B_2$ of two 3-balls and there is a local system of coordinates for $B \cong \mathbb{R}^4$, such that
$$\begin{cases} \varphi(B_1) = \left\{ \left(t, r\cos(s), r\sin(s), 0\right) \;\middle|\; t,s \in \mathbb{R}, r \in [0,2] \right\} \\ \varphi(B_2) = \left\{ \left(0, r\cos(s), r\sin(s), t\right) \;\middle|\; t,s \in \mathbb{R}, r \in [0,1] \right\} \end{cases};$$
- *of type* 2 if $\varphi^{-1}(B)$ is the disjoint union $B_1 \sqcup B_2$ of two 3-balls and there is a local system of coordinates for $B \cong \mathbb{R}^4$, such that
$$\begin{cases} \varphi(B_1) = \left\{ \left(t, r\cos(s), r\sin(s), t^2\right) \;\middle|\; t,s \in \mathbb{R}, r \in [0,2] \right\} \\ \varphi(B_2) = \left\{ \left(t, r\cos(s), r\sin(s), -t^2\right) \;\middle|\; t,s \in \mathbb{R}, r \in [0,1] \right\} \end{cases};$$
- *of type* 3 if $\varphi^{-1}(B)$ is the disjoint union $B_1 \sqcup B_2 \sqcup B_3$ of three 3-balls and there is a local system of coordinates for $B \cong \mathbb{R}^4$, such that
$$\begin{cases} \varphi(B_1) = \left\{ \left(t, r\cos(s), r\sin(s), 0\right) \;\middle|\; t,s \in \mathbb{R}, r \in [0,2] \right\} \\ \varphi(B_2) = \left\{ \left(t, r\cos(s), r\sin(s), t\right) \;\middle|\; t,s \in \mathbb{R}, r \in [0,1] \right\} \\ \varphi(B_3) = \left\{ \left(t, r\cos(s), r\sin(s), -t\right) \;\middle|\; t,s \in \mathbb{R}, r \in \left[0, \tfrac{1}{2}\right] \right\} \end{cases};$$
- *of type* SV if $\varphi^{-1}(B)$ is the disjoint union $B_1 \sqcup B_2$ of two 3-balls, B_1 and B_2 belong to the same connected component of M, and there is a local system of coordinates for $B \cong \mathbb{R}^4$, such that $\begin{cases} \varphi(B_1) = \left\{ \left(r, t, s, 0\right) \;\middle|\; t,s \in \mathbb{R}, r \in \mathbb{R}_- \right\} \\ \varphi(B_2) = \left\{ \left(0, r\cos(s), r\sin(s), t\right) \;\middle|\; t,s \in \mathbb{R}, r \in [0,1], r \right\} \end{cases}$.

Remark 3.2. In all four cases, the ribbon singularity D corresponds to the disk $\left\{ \left(0, r\cos(s), r\sin(s), 0\right) \;\middle|\; s \in \mathbb{R}, r \in [0,1] \right\}$. Type 0 corresponds to two solid tubes, one being smaller than the other, intersecting transversally; these are the usual ribbon singularities. Type 2 corresponds to two solid tubes, one being smaller than the other, intersecting tangentially; these occur when spinning a link around a plane on which the link projects

[3]For the sake of exactitude, we provide here explicit formulas for the singularities, but informal descriptions follow in Remark 3.2.

https://doi.org/10.1017/S1474748023000543 Published online by Cambridge University Press

with two tangential strands. Type 3 corresponds to three solid tubes of increasing width, intersecting simultaneously and transversally; these occur when spinning a link around a plane on which the link projects with a triple point. Type SV differs from type 0 in that one preimage of the singular disk lies on the boundary of M instead of its interior, and in that the two preimages belong to the same solid torus; these occur when performing the link-homotopy which pushes at once a usual ribbon (self) singularity through the boundary of M. Note that a type 1 seems to be missing here, which would correspond to spinning a link around a plane on which the link projects with a cusp, but this does not introduce any new kind of ribbon singularity.

Definition 3.3. *Ribbon solid tori* are immersions of a finite number of solid tori in S^4 whose singular locus consists of ribbon singularities of type 0. *Generalized ribbon solid tori* are immersed solid tori in S^4 whose singular locus is made of ribbon singularities of type 0, 2, and 3. *Self-singular ribbon solid tori* are immersed solid tori in S^4 whose singular locus is made of ribbon singularities of type 0 and SV.

We say that two (generalized) ribbon solid tori are *equivalent* if there is a path among generalized ribbon solid tori connecting them, and we say that they are *ribbon link-homotopic* if there is a path among generalized and self-singular ribbon solid tori connecting them.

Remark 3.4. Note that generalized ribbon solid tori may have singularities between distinct components, but that the boundary of the solid tori is embedded, while the boundary of self-singular ribbon solid tori may have double points within a same component.

Adding the spun of projection rays in the above definition of the Spun map provides a well-defined map $\mathrm{Spun}^\bullet$ from classical links to generalized ribbon solid tori. The following result is the topological characterization of the reduced peripheral system given by the equivalence i $\Leftrightarrow$ iii in our main theorem.

Theorem 3.5. *Two classical links L and L' have isomorphic reduced peripheral systems if and only if* $\mathrm{Spun}^\bullet(L)$ *and* $\mathrm{Spun}^\bullet(L')$ *are ribbon link-homotopic.*

The proof is given in the next section. As for the diagrammatic characterization given in Section 2, this will follow from a more general result, Theorem 3.7, characterizing the reduced peripheral system of welded links in terms of 4-dimensional topology.

3.2. The enhanced Tube map

In this section, we prove Theorem 3.5, using the so-called Tube map. Recall from [20] that Satoh's generalization of Yajima's Tube map is defined from welded links to ribbon knotted 2-tori, and that for any welded link L, $\mathrm{Tube}(L)$ actually comes with a canonical ribbon filling. In order to fully record this ribbon filling in the Tube map, and to connect with the $\mathrm{Spun}^\bullet$ map, we are led to the following notion.

https://doi.org/10.1017/S1474748023000543 Published online by Cambridge University Press

Definition 3.6. We define *generalized welded diagrams* as diagrams with cusps and the following kind of crossings:

Then classical Reidemeister moves are replaced by a path of diagrams going through the corresponding cusp, tangential or triple point. Other welded moves are still locally allowed.

We define *self-singular welded diagrams* as diagrams with the following kind of crossings, where the two strands involved in a semi-virtual crossing belong to a same component[4]:

Self-virtualization is defined for generalized welded diagrams as the equivalence relation generated by the local moves turning a semi-virtual crossing into either a classical crossing, or a virtual one as follows:

Following [3, Section 3.2], one can then define a map

$$\mathrm{Tube}^{\bullet} : \frac{\{\text{generalized welded diagrams}\}}{\text{self-virtualization}} \to \frac{\{\text{generalized ribbon solid tori}\}}{\text{ribbon link-homotopy}}$$

which, respectively, associates ribbon singularities of type 0, 2, 3, and SV to classical, tangential, triple, and semi-virtual crossings and connects these various singularities by pairwise disjoint 3-balls, as prescribed combinatorially by the welded diagram. It is then a straightforward adaptation of [3, Proposition 3.7] to prove that $\mathrm{Tube}^{\bullet}$ is one-to-one. More precisely, in the terminology of [3], the case $d = 2$ of Proposition 3.7 states that Conn map, from 3-ribbons to welded diagrams, is an isomorphism. Here, 3-*ribbons* are 3-dimensional ribbon balls in B^4 attached to ∂B^4 by disks (they are to ribbon solid tori what string-links are to links), and Conn is the inverse function of $\mathrm{Tube}^{\bullet}$, which associates a welded diagram to any 3-ribbon by encoding the way ribbon singularities are attached one to the others. The key point is to prove that Conn is injective, and this is done by considering standard neighborhoods $\{U_i\}$ for the ribbon singularities, and showing that, up to isotopy, there is a unique way to embed regular tubes in $B^4 \setminus \{U_i\}$ to connect them: the exact same argument applies in the case of generalized ribbon solid tori.

[4]Semi-virtual crossings were already introduced in [11] in connection with finite type invariants of virtual knots.

https://doi.org/10.1017/S1474748023000543 Published online by Cambridge University Press

As a direct corollary of Theorem 2.1, we obtain the following alternative characterization of the reduced peripheral system, which holds for all welded links.

Theorem 3.7. *Two welded links L_1 and L_2 have isomorphic reduced peripheral systems if and only if* $\mathrm{Tube}^\bullet(L_1)$ *and* $\mathrm{Tube}^\bullet(L_2)$ *are ribbon link-homotopic.*

Theorem 3.5 follows from this result. Indeed, as essentially pointed out by Satoh in [20], it is clear from the definition of the $\mathrm{Spun}^\bullet$ map that, if D is a diagram of a classical link L, the ribbon solid tori $\mathrm{Spun}^\bullet(L)$ consists of ribbon singularities which are connected by 3-balls as combinatorially prescribed by D: $\mathrm{Spun}^\bullet(L)$ and $\mathrm{Tube}^\bullet(L)$ are hence equivalent.

3.3. Link-homotopy of ribbon surfaces in 4-space

The original versions of the Spun and Tube maps produce ribbon 2-tori, which are just the boundary of some ribbon solid tori, rather than 3-dimensional objects. Obviously, any ribbon link-homotopy between two ribbon solid tori induces a usual link-homotopy between their boundaries. Building on this remark, it follows that:

Proposition 3.8. *If two classical links L_1 and L_2 have isomorphic reduced peripheral systems, then* $\mathrm{Spun}(L_1)$ *and* $\mathrm{Spun}(L_2)$ *are link-homotopic.*

It is hence tempting to hope for the converse to hold true: this would give a topological characterization of the reduced peripheral system in terms of spun surfaces up to link-homotopy. However, this is not the case. There is indeed a known global move on welded links, related to the torus eversion in S^4, under which the Spun map is invariant, and this move transforms every classical link into its *reversed image*, which is the mirror image with reversed orientation (see [22] or [2, Proposition 2.7]). Furthermore, it can be checked that the (reduced) peripheral system of a reversed image is given from the initial one by just inverting the longitudes. It follows easily from these two observations that, for instance, the positive and negative Hopf links have nonequivalent reduced peripheral systems, whereas their spuns are isotopic, hence link-homotopic. As a consequence, keeping track of the ribbon filling is mandatory to preserve (reduced) peripheral systems, and Theorem 3.5 is in this sense optimal.

Acknowledgments. The authors thank A. Yasuhara for useful comments on earlier versions of this paper.

Competing interest. The authors have no competing interest to declare.

References

[1] E. Artin, Zur isotopie zweidimensionalen flächen im R_4, *Abh. Math. Sem. Univ. Hamburg*, **4** (1926), 174–177.

[2] B. Audoux, On the welded tube map, in Knot theory and its applications, *Contemporary Mathematics*, vol 670, pp. 261–284 (American Mathematical Society, Providence, RI, 2016).

[3] B. Audoux, *Applications de modèles combinatoires issus de la topologie*. Habilitation, Aix–Marseille University, 2018.
[4] B. Audoux, P. Bellingeri, J.-B. Meilhan and E. Wagner, Homotopy classification of ribbon tubes and welded string links, *Ann. Sc. Norm. Super. Pisa Cl. Sci.* **17**(1) (2017), 713–761.
[5] D. Bar-Natan and Z. Dancso, Finite type invariants of w-knotted objects. II: Tangles, foams and the Kashiwara-Vergne problem, *Math. Ann.* **367**(3–4) (2017), 1517–1586.
[6] D. Bar-Natan, Z. Dancso and N. Scherich, Ribbon 2-knots, $1+1=2$ and Duflo's theorem for arbitrary Lie algebras, *Algebr. Geom. Topol.* **20**(7) (2020), 3733–3760.
[7] B. Colombari, A diagrammatic characterization of Milnor invariants, *Preprint*, 2021, https://arxiv.org/abs/2201.01499.
[8] J. Conant, R. Schneiderman and P. Teichner, Milnor invariants and twisted Whitney towers, *J. Top.* **7**(1) (2014), 187–224.
[9] C. Damiani, A journey through loop braid groups, *Expositiones Mathematicae* **35**(3) (2017), 252–285.
[10] R. Fenn, R. Rimányi and C. Rourke, The braid-permutation group, *Topology* **36**(1) (1997), 123–135.
[11] M. Goussarov, M. Polyak and O. Viro, Finite-type invariants of classical and virtual knots, *Topology* **39**(5) (2000), 1045–1068.
[12] N. Habegger and X.-S. Lin, The classification of links up to link-homotopy, *J. Amer. Math. Soc.* **3** (1990), 389–419.
[13] J. R. Hughes, Structured groups and link-homotopy, *J. Knot Theory Ramifications* **2**(1) (1993), 37–63.
[14] L. H. Kauffman, Virtual knot theory, *European J. Combin.* **20**(7) (1999), 663–690.
[15] S.-G. Kim, Virtual knot groups and their peripheral structure, *J. Knot Theory Ramifications* **9**(6) (2000), 797–812.
[16] J. P. Levine, An approach to homotopy classification of links, *Trans. Am. Math. Soc.* **306**(1) (1988), 361–387.
[17] J.-B. Meilhan and A. Yasuhara, Arrow calculus for welded and classical links, *Alg. Geom. Topol.* **19**(1) (2019), 397–456.
[18] J. Milnor, Link groups, *Ann. of Math. (2)* **59** (1954), 177–195.
[19] J. Milnor, Isotopy of links, in Algebraic geometry and topology, A symposium in honor of Solomon Lefschetz, *Princeton Legacy Library*, pp. 280–306 (Princeton University Press, Princeton, N. J., 1957).
[20] S. Satoh, Virtual knot presentation of ribbon torus-knots, *J. Knot Theory Ramifications* **9**(4) (2000), 531–542.
[21] F. Waldhausen, On irreducible 3-manifolds which are sufficiently large, *Ann. Math. (2)* **87** (1968), 56–88.
[22] B. Winter, The classification of spun torus knots, *J. Knot Theory Ramifications* **18**(9) (2009), 1287–1298.

Appendix. Hughes's counterexample

As mentioned in the Introduction, the fact that the reduced peripheral system of classical links is not a complete link-homotopy invariant was made explicit by Hughes in [13]. There, a pair of 4-component links is given, which have isomorphic reduced peripheral systems but are not link-homotopic; this latter fact is proved using Levine's refinement of Milnor invariants developed in [16]. These two links, H_1 and H_2, are given by the closures of the following pure braids, oriented from left to right:

https://doi.org/10.1017/S1474748023000543 Published online by Cambridge University Press

H_1 :

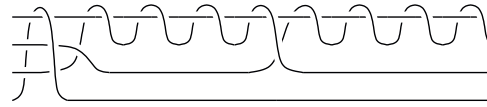

;

H_2 :

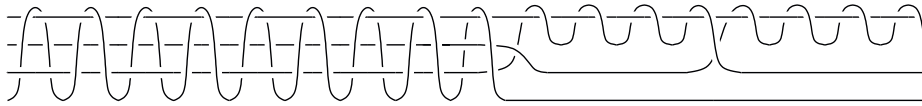

.

Our main theorem implies that, although not link-homotopic, the links H_1 and H_2 are sv-equivalent. This fact, however, is rather difficult to verify by hand, and we outline in this appendix the method that we used for this verification.

We make use of the theory of *arrow calculus* developed in [17], which is in some sense a "higher order Gauss diagram" theory. We only give here a quick overview of this theory, and refer to [17] for precisions and further details. Roughly speaking, a w-arrow for a diagram L is an oriented interval, possibly decorated by a dot, immersed in the plane so that the endpoints lie on L; one can perform *surgery* on L along this w-arrow to obtain a new diagram as follows:

More generally, one defines w-trees, which are oriented unitrivalent trees defined recursively by the rules:

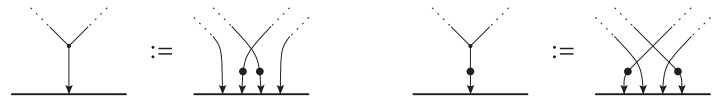

There, the dotted parts represent "parallel" subtrees, see [17, Convention 5.1]. Any welded diagram can be represented as a diagram without any crossing, but with w-trees. For example, the links H_1 and H_2 can be represented in this way as the closures of the diagrams given in Figure 4 (ignoring the integer labels). Note that the presentation for H_2 only differs from that for H_1 by the addition of a union Y of Y–shaped w-trees.

It is shown in [17, Sections 4–5] that two dots on a same edge do cancel, and that the following moves can be performed on w-trees:

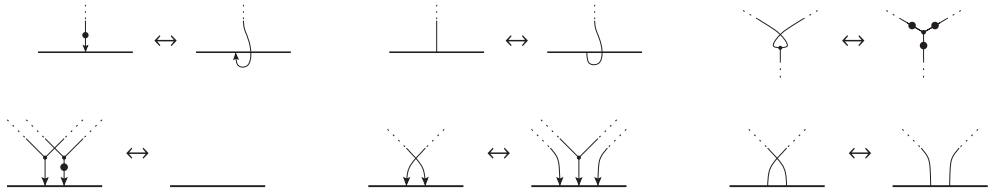

Moreover, up to sv-equivalence, it is shown in [17, Section 9] that so-called *repeated* w-trees having at least two endpoints on a same connected component can be removed,

https://doi.org/10.1017/S1474748023000543 Published online by Cambridge University Press

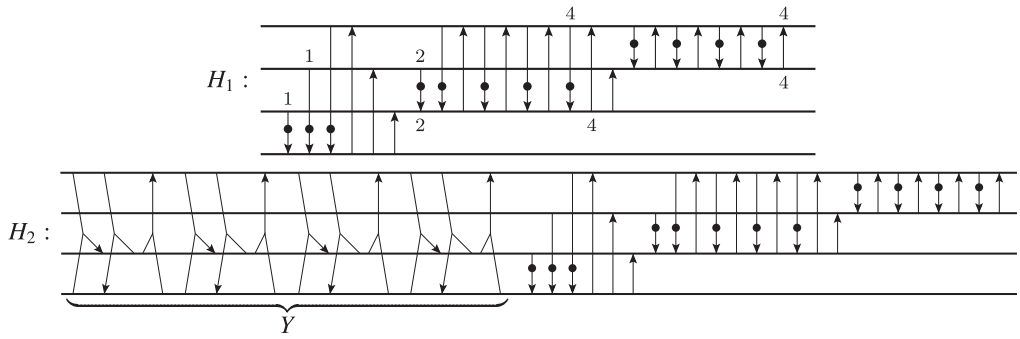

Figure 4. Arrow presentations of Hughes's links H_1 and H_2.

and that the following moves can also be performed:

Then, one can start with the diagram for H_1 given in Figure 4, pick some w-arrow endpoint, and slide it all around the component it is attached to, in either direction: by the above moves, this will create Y-shaped w-trees, which can in turn be "gathered" at the cost of higher order w-trees. By performing the appropriate sequence of slides and cancelling inverse pairs and repeated w-trees, one can create the union Y of w-trees realizing the presentation for H_2, thus showing that the two links H_1 and H_2 are indeed sv-equivalent. Such an appropriate sequence of slides is indicated in the upper part of Figure 4: there, an integer label k (respectively, $\overline{k}$) near an arrow end indicates k full turns in the left (respectively, right) direction.

https://doi.org/10.1017/S1474748023000543 Published online by Cambridge University Press